Supplementary Information

Unexpected Quasi-Alternating Copolymerization of Oxiranes Driven by a Benign Acetate-based Catalyst

Charlotte Fornaciari[1,2], Vincent Lemaur[3], Dario Pasini[2]*, Olivier Coulembier[1]*

[1] Laboratory of Polymeric and Composite Materials (LPCM), Center of Innovation and Research in Materials and Polymers (CIRMAP), University of Mons, Place du Parc, 20, Mons 7000, Belgium.

[2] Department of Chemistry, University of Pavia, Viale Taramelli, 10, Pavia 27100, Italy.

[3] Laboratory for Chemistry of Novel Materials, Center for Innovation and Research in Materials and Polymers (CIRMAP), University of Mons, Place du Parc, 20, 7000 Mons, Belgium.

E-mail: olivier.coulembier@umons.ac.be

dario.pasini@unipv.it

Table of Contents

1. Supplementary Methods

1.1. Materials

Propylene oxide (PO, ≥ 99%, Aldrich) and allyl glycidyl ether (AGE, ≥ 99%, Aldrich) were dried over CaH_2, distilled and stored over molecular sieves. Benzyl alcohol (BnOH) and isopropyl alcohol (iPrOH) were dried over CaH_2 for 48 hours prior to their distillation under reduced pressure. Potassium acetate (KOAc, ≥ 99%, VWR) was dried by heating at 100 °C under vacuum for 48 hours. 18-Crown ether-6 (18C6, 99%, ACROS Organics) was dried by three azeotropic distillations of tetrahydrofuran (THF). Compounds were all stored in a glove box (O_2 ≤ 6 ppm, H_2O ≤ 1 ppm). THF solvent was dried using a MBraun Solvent Purification System (model MB-SPS 800) equipped with alumina drying columns.

1.2. General techniques

^1H and ^{13}C nuclear magnetic resonance (NMR) spectra were recorded using a Bruker AVANCEII 500 MHz apparatus and a Bruker Avance III 400 MHz spectrometer at room temperature in chloroform-d_1 ($CDCl_3$). All spectra were acquired according to the following parameters: aq = 6.8 sec, d1 = 10 sec, sw = 12, o1p = 5, ns = 128 (4000 for ^{13}C), PULPROG zg30. Size exclusion chromatography (SEC) was performed in THF at 35 °C using a Triple Detection Polymer Laboratories liquid chromatograph equipped with a refractive index (ERMA 7517), a UV detector (254 nm), a capillary viscometry, a light scattering RALS (Viscotek T-60) (Polymer Laboratories GPC-RI/CV / RALS) and an automatic injector (Polymer Laboratories GPC-RI/UV) and four columns : a PL gel 10 µm guard column and three PL gel Mixed-B 10 µm columns (linear columns for separation of MwPS ranging from 500 to 10^6 daltons). Positive-ion MALDI-Mass Spectrometry (MALDI-MS) experiments were recorded using a Waters QToF Premier mass spectrometer equipped with a Nd:YAG (third harmonic) operating at 355 nm with a maximum output of 65 µJ delivered to the sample in 2.2 ns pulses at 50 Hz repeating rate. Time-of-flight mass analyses were performed in the reflectron mode at a resolution of about 10,000. All the samples were analyzed using trans-2-[3-(4-tert-butylphenyl)-2-methylprop-2-enylidene]malononitrile (DCTB) as matrix. That matrix was prepared as 40 $mg.mL^{-1}$ solution in $CHCl_3$. The matrix solution (1 µL) was applied to a stainless steel target and air-dried. Polymer samples were dissolved in THF to obtain 1 $mg.mL^{-1}$ solutions. Therefore, 1 µL of this solution was applied onto the target area already bearing the matrix crystals, and air-dried. For the recording of the single-stage MS spectra, the quadrupole (rf-only mode) was set to pass all the ions of the distribution, and they were transmitted into the pusher region of the time-of-flight analyzer where they were mass analyzed with 1s integration time. Data were acquired in continuum mode until acceptable averaged data were obtained. Molecular mechanics and molecular dynamics simulations have been performed with the COMPASSIII force field as implemented in the BIOVIA Materials Studio 2022 package. In practice, adducts and the

18C6/KOAc complex have been put in contact and then subjected to a geometry optimization followed by successive 5-ns long quenched dynamics (NVT; quench every 5 ps) at increasing temperature (T = 300K, 400K, 600K and 1000K). At each temperature, multiple quenched dynamics runs have been performed until energy convergence between two successive runs is reached. Finally, the impact of the presence of the initiator on the interactions between the propagating monomer and the acetate has been evaluated from the distance measurements between the hydrogen of the hydroxyl group of the propagating monomer and the oxygen of the acetate.

1.3. Synthesis and Characterization

1.3.1. General Procedure for PO Homopolymerization from BnOH

In a glove box, a vial equipped with a stir bar was charged with BnOH (21 mg, 0.194 x 10^{-3} mol), KOAc (9.4 mg, 0.096 x 10^{-3} mol), 18C6 (25.5 mg, 0.096 x 10^{-3} mol), and PO (281 mg, 4.8 x 10^{-3} mol). The reaction is then performed at 21 °C and kinetically studied by SEC analysis and ^{1}H NMR spectroscopy.

^{1}H NMR ($CDCl_3$, 400 MHz): δ 1.07-1.14 (m, −C<u>H</u>$_3$), 3.32−3.60 (broad m, −O−C<u>H</u>$_2$−C<u>H</u>(CH_3)−O−), 4.54 (s, Ph−C<u>H</u>$_2$−O−), 7.17−7.33 (broad m, <u>Ph</u>−CH_2−O−). ^{13}C NMR ($CDCl_3$, 101 MHz): δ 17.45 (−<u>C</u>H_3), 73.09 (−O−<u>C</u>H_2−CH(CH_3)−O−, rrm or mrr), 73.42 (−O−<u>C</u>H_2−CH(CH_3)−O−, m), 75.23 (−O−CH_2− <u>C</u>H(CH_3)−O−, rr), 75.47 (−O−CH_2−<u>C</u>H(CH_3)−O−, mr + rm), 75.66 (−O−CH_2−<u>C</u>H(CH_3)−O−, mm), 127.65/127.60/128.46/138.59 (<u>Ph</u>−CH_2−O−).

1.3.2. General Procedure for AGE Homopolymerization from BnOH

In a glove box, a vial equipped with a stir bar was charged with BnOH (21 mg, 0.194 x 10^{-3} mol), KOAc (9.4 mg, 0.096 x 10^{-3} mol), 18C6 (25.5 mg, 0.096 x 10^{-3} mol), and AGE (554 mg, 4.8 x 10^{-3} mol). The reaction is then performed at 21 °C and kinetically studied by SEC analysis and ^{1}H NMR spectroscopy.

^{1}H NMR ($CDCl_3$, 400 MHz): δ 3.40−3.67 (broad m, −O−C<u>H</u>$_2$−C<u>H</u>(C<u>H</u>$_2$−O−CH_2−CH=CH_2)−O−), 3.97-3.98 (d, −O−C<u>H</u>$_2$−CH=CH_2), 4.53 (s, −Ph−C<u>H</u>$_2$−O−), 5.13-5.27 (doublet of doublets, −O−CH_2−CH=C<u>H</u>$_2$), 5.84-5.89 (m, −O−CH_2−C<u>H</u>=CH_2), 7.32 (broad m, <u>Ph</u>−CH_2−O−). ^{13}C NMR ($CDCl_3$, 101 MHz): δ 69.92 (−O−<u>C</u>H_2−CH(CH_2−O−CH_2−CH=CH_2)−O−, rrm or mrr), 69.31−70.35 (−O−<u>C</u>H_2−CH(<u>C</u>H_2−O−CH_2−CH=CH_2)−O−, m), 72.39 (−O−<u>C</u>H_2−CH=CH_2), 78.94 (−O−CH_2−CH(CH_2−O−CH_2−<u>C</u>H=CH_2)−O−), 116.85 (−O−CH2−CH=<u>C</u>H_2), 127.69/127.71/128.48/138.46 (<u>Ph</u>−CH_2−O−), 134.89 (−O−CH_2−<u>C</u>H=CH_2).

1.3.3. General Procedure for PO S_N2 Reaction with BnOH.

In a glove box, a vial equipped with a stir bar was charged with BnOH (100 mg, 0.92 x 10^{-3} mol), KOAc (45 mg, 0.46 x 10^{-3} mol), 18C6 (122 mg, 0.46 x 10^{-3} mol), and PO (107 mg, 1.84 x 10^{-3} mol).

The reaction is then performed at 21 °C and kinetically studied by SEC analysis and ^{1}H NMR spectroscopy.

^{1}H NMR ($CDCl_3$, 500 MHz): δ 1.07-1.14 (m, −C<u>H</u>$_3$), 3.27−3.48 (m, −O−C<u>H</u>$_2$−C<u>H</u>(CH$_3$)−O−), 4.55 (s, Ph−C<u>H</u>$_2$−O−), 7.33 (broad m, <u>Ph</u>−CH$_2$−O−).

1.3.4. General Procedure for Copolymerization of PO and AGE from BnOH.

In a glove box, a vial equipped with a stir bar was charged with BnOH, KOAc, 18C6, PO and AGE. All copolymerizations were carried out in bulk at r.t. by targeting a degree of polymerization (DP = [PO+AGE]$_0$/[BnOH]$_0$) of 25 and varying the initial monomer composition (F = [PO]$_0$/[AGE]$_0$). The polymerization kinetics were determined by ^{1}H NMR spectroscopy in function of time.

^{1}H NMR ($CDCl_3$, 400 MHz): δ 1.12 (m, −C<u>H</u>$_3$), 3.40−3.70 (broad m, (−O−C<u>H</u>$_2$−C<u>H</u>(CH$_3$)−O− and −O−C<u>H</u>$_2$−C<u>H</u>(C<u>H</u>$_2$−O−CH$_2$−CH=CH$_2$)−O−), 3.99 (d, −O−C<u>H</u>$_2$−CH=CH$_2$), 4.53-4.54 (s, −Ph−C<u>H</u>$_2$−O−), 5.13-5.27 (doublet of doublets, −O−CH$_2$−CH=C<u>H</u>$_2$), 5.84-5.89 (m, −O−CH$_2$−C<u>H</u>=CH$_2$), 7.32 (broad m, <u>Ph</u>−CH$_2$−O−). ^{13}C NMR ($CDCl_3$, 101 MHz): δ 17.46 (−<u>C</u>H$_3$), 69.33/70.36 (−O−<u>C</u>H$_2$−CH(<u>C</u>H$_2$−O−CH$_2$−CH=CH$_2$)−O−), 72.40 (−O−<u>C</u>H$_2$−CH=CH$_2$), 73.50/74.45 (−O−<u>C</u>H$_2$−CH(CH$_3$)−O−), 75.47 (−O−CH$_2$−<u>C</u>H(CH$_3$)−O−), 78.94 (−O−CH$_2$−<u>C</u>H(CH$_2$−O−CH$_2$−CH=CH$_2$)−O−), 116.84 (−O−CH$_2$−CH=<u>C</u>H$_2$), 127.66/127.70/128.47/138.47 (<u>Ph</u>−CH$_2$−O−), 134.92 (−O−CH$_2$−<u>C</u>H=CH$_2$).

2. Supplementary Tables

***F* = 0.1**

REAGENTS	eqv.	mol	amount
PO	2.3	0.44 x 10^{-3}	0.026 g
AGE	22.7	4.4 x 10^{-3}	0.502 g
BnOH	1	0.194 x 10^{-3}	0.021 g
KOAc	0.5	0.096 x 10^{-3}	0.0094 g
18C6	0.5	0.096 x 10^{-3}	0.0255 g

***F* = 0.2**

REAGENTS	eqv.	mol	amount
PO	4.2	0.84 x 10^{-3}	0.049 g
AGE	20.8	4.2 x 10^{-3}	0.480 g
BnOH	1	0.2 x 10^{-3}	0.0219 g
KOAc	0.5	0.096 x 10^{-3}	0.0095 g
18C6	0.5	0.097 x 10^{-3}	0.0258 g

***F* = 0.31**

REAGENTS	eqv.	mol	amount
PO	6	1.17×10^{-3}	0.068 g
AGE	19	3.7×10^{-3}	0.426 g
BnOH	1	0.194×10^{-3}	0.021 g
KOAc	0.5	0.096×10^{-3}	0.0094 g
18C6	0.5	0.096×10^{-3}	0.0256 g

***F* = 0.75**

REAGENTS	eqv.	mol	amount
PO	10.7	2.17×10^{-3}	0.126 g
AGE	14.3	2.9×10^{-3}	0.340 g
BnOH	1	0.2×10^{-3}	0.022 g
KOAc	0.5	0.096×10^{-3}	0.0095 g
18C6	0.5	0.096×10^{-3}	0.0255 g

***F* = 1**

REAGENTS	eqv.	mol	amount
PO	12.5	2.4×10^{-3}	0.142 g
AGE	12.5	2.4×10^{-3}	0.277 g
BnOH	1	0.194×10^{-3}	0.021 g
KOAc	0.5	0.096×10^{-3}	0.0095 g
18C6	0.5	0.096×10^{-3}	0.0254 g

***F* = 2.06**

REAGENTS	eqv.	mol	amount
PO	16.8	3.3×10^{-3}	0.196 g
AGE	8.2	1.6×10^{-3}	0.185 g
BnOH	1	0.196×10^{-3}	0.0213 g
KOAc	0.5	0.096×10^{-3}	0.0095 g
18C6	0.5	0.096×10^{-3}	0.0254 g

***F* = 5.06**

REAGENTS	eqv.	mol	amount
PO	21	4×10^{-3}	0.237 g
AGE	4	0.79×10^{-3}	0.091 g
BnOH	1	0.194×10^{-3}	0.021 g
KOAc	0.5	0.096×10^{-3}	0.0094 g
18C6	0.5	0.096×10^{-3}	0.255

3. Supplementary Figures

3.1. Kinetics of PO and AGE homopolymerizations with BnOH.

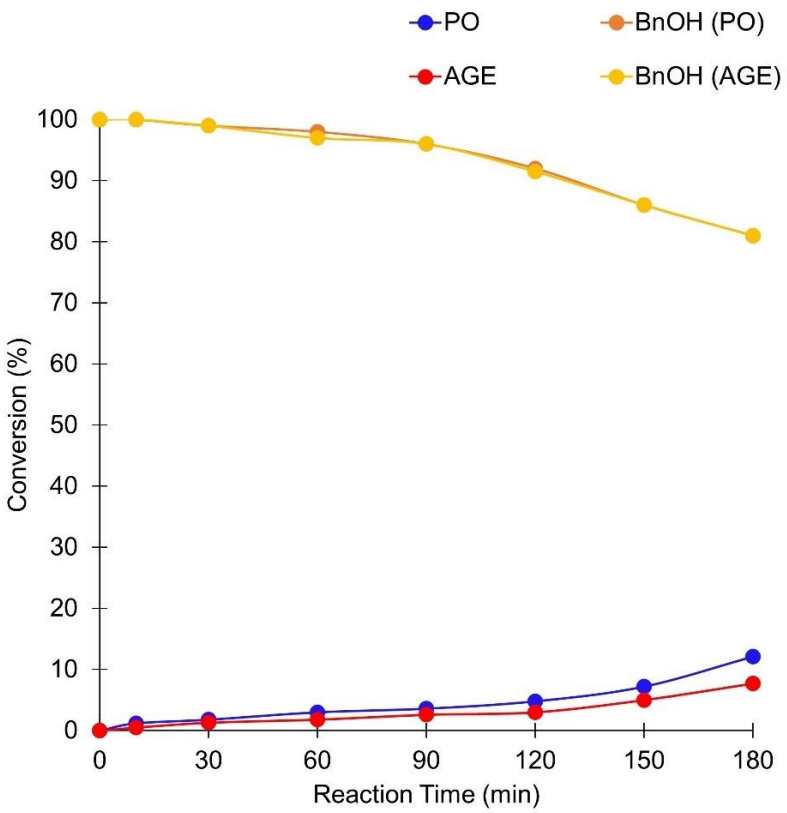

Supplementary Figure 1. Kinetics of PO and AGE homopolymerizations with BnOH activated by 18C6/KOAc complex. Conditions: $[M]_0/[BnOH]_0/[18C6/KOAc]_0 = 25/1/0.5$.

3.2. SEC traces of product obtained by PO S_N2 reaction.

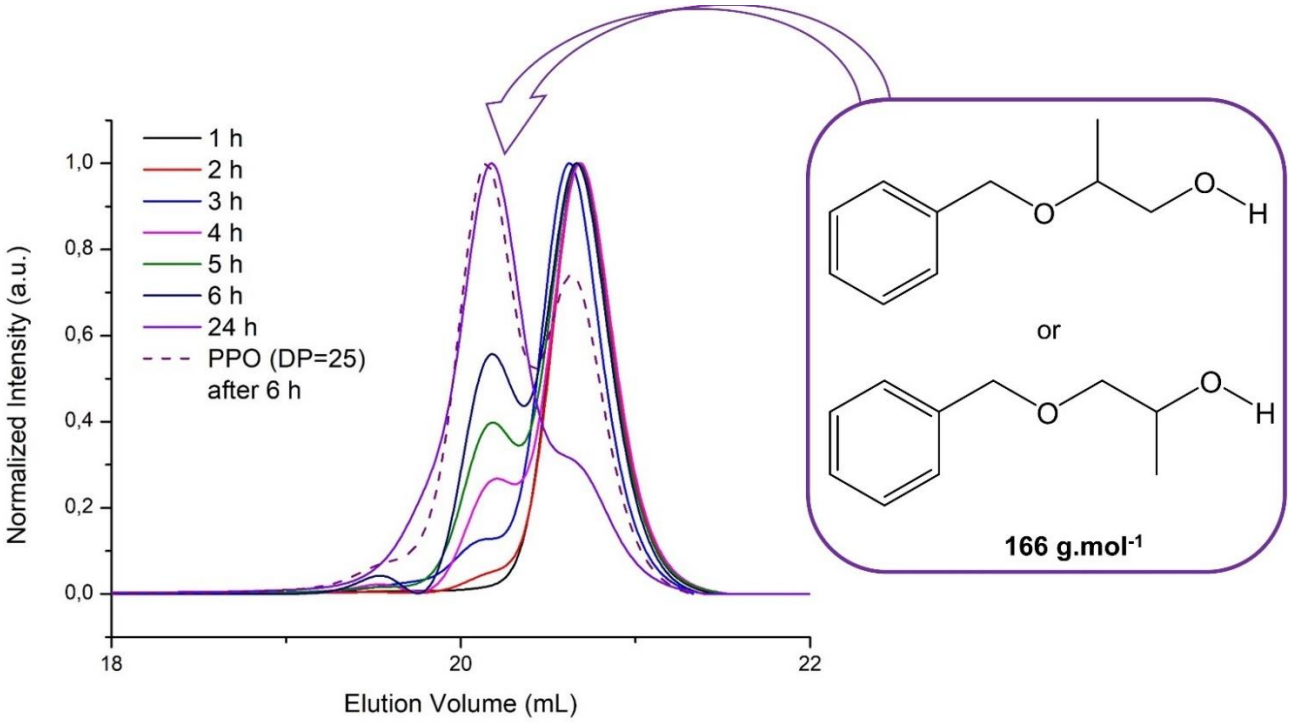

Supplementary Figure 2. Evolution of SEC traces of the crude product between PO and BnOH with the time. Conditions: $[PO]_0/[BnOH]_0/[18C6/KOAc]_0$ = 2/1/0.5.

3.3. ^{1}H NMR spectrum of product between PO and BnOH.

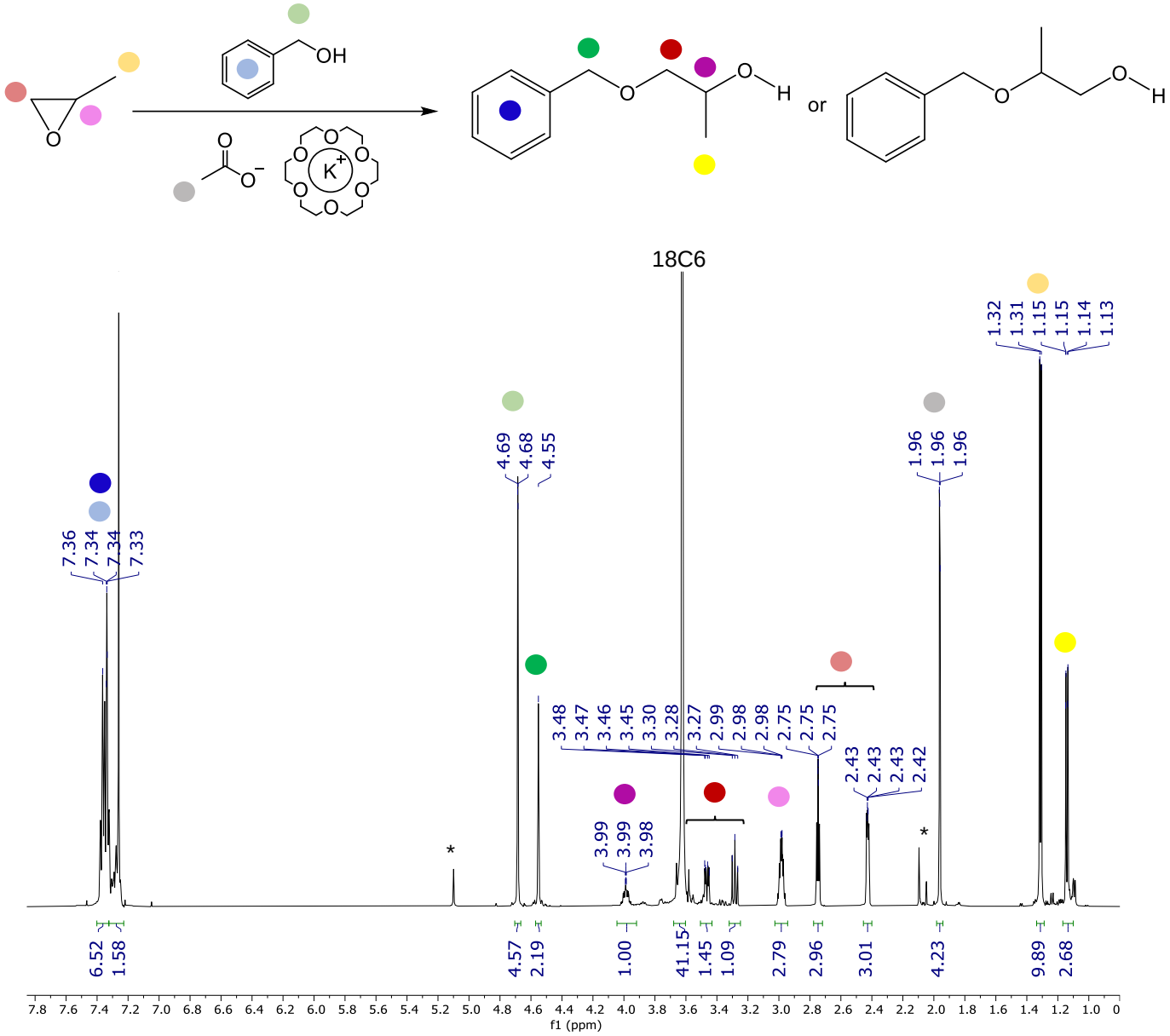

Supplementary Figure 3. ^{1}H NMR spectrum ($CDCl_3$, 500 MHz) of the crude product between BnOH and PO activated by 18C6/KOAc complex after 6 h. Condition: $[PO]_0/[BnOH]_0/[18C6/KOAc]_0$ = 2/1/0.5. (*) Signals associated to the presence of impurities in the crude products.

3.4. ^{1}H and ^{13}C NMR spectra of PPO.

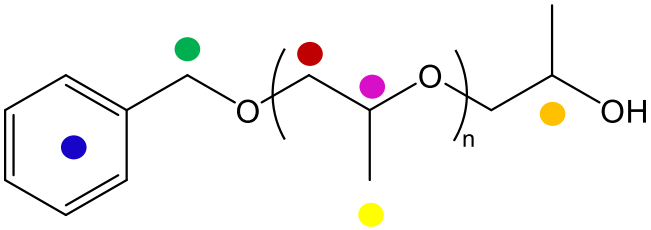

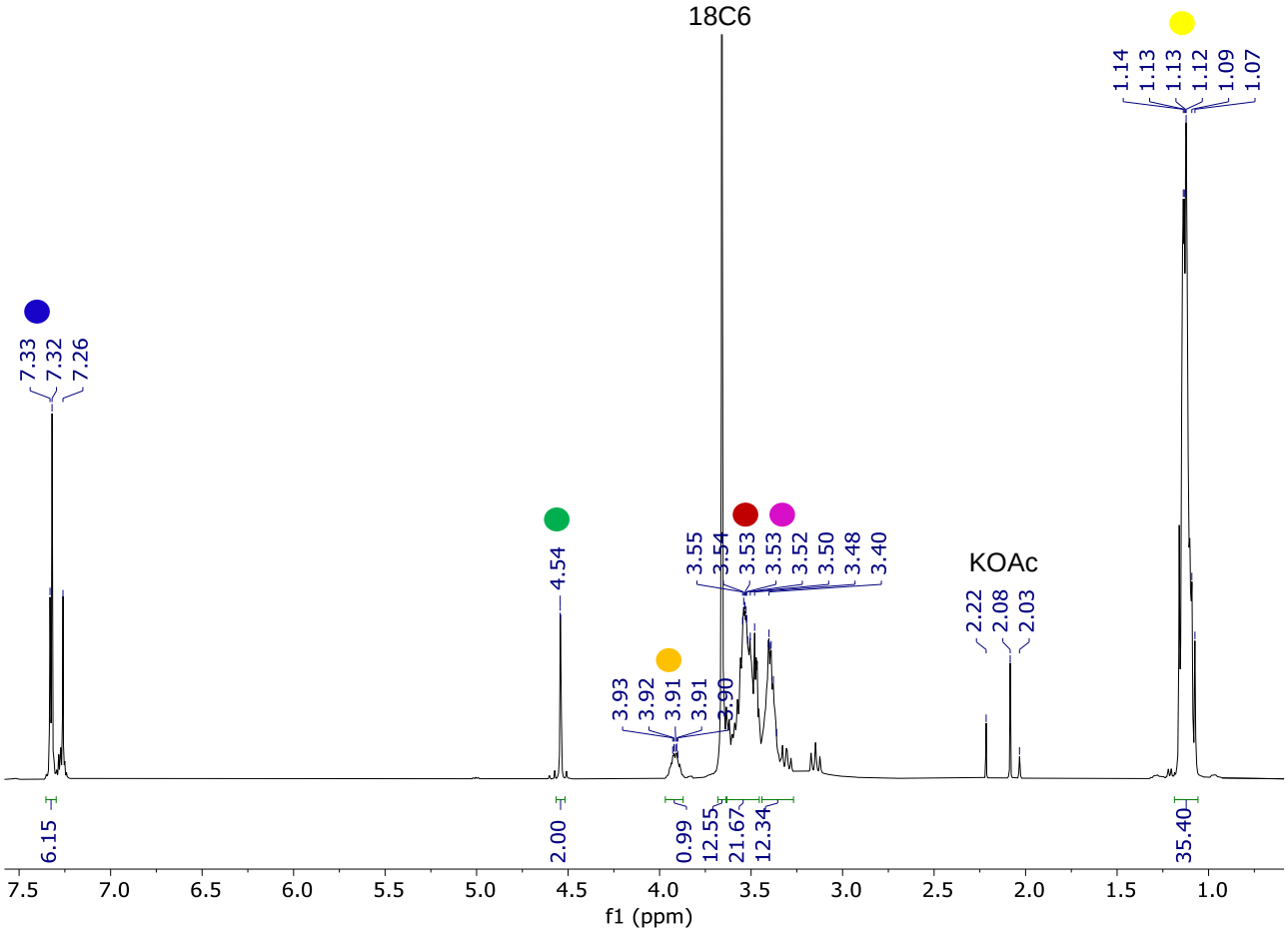

Supplementary Figure 4. ^{1}H NMR spectrum ($CDCl_3$, 400 MHz) of the crude PPO after full conversion. Condition: $[PO]_0/[BnOH]_0/[18C6/KOAc]_0$ = 25/1/0.5.

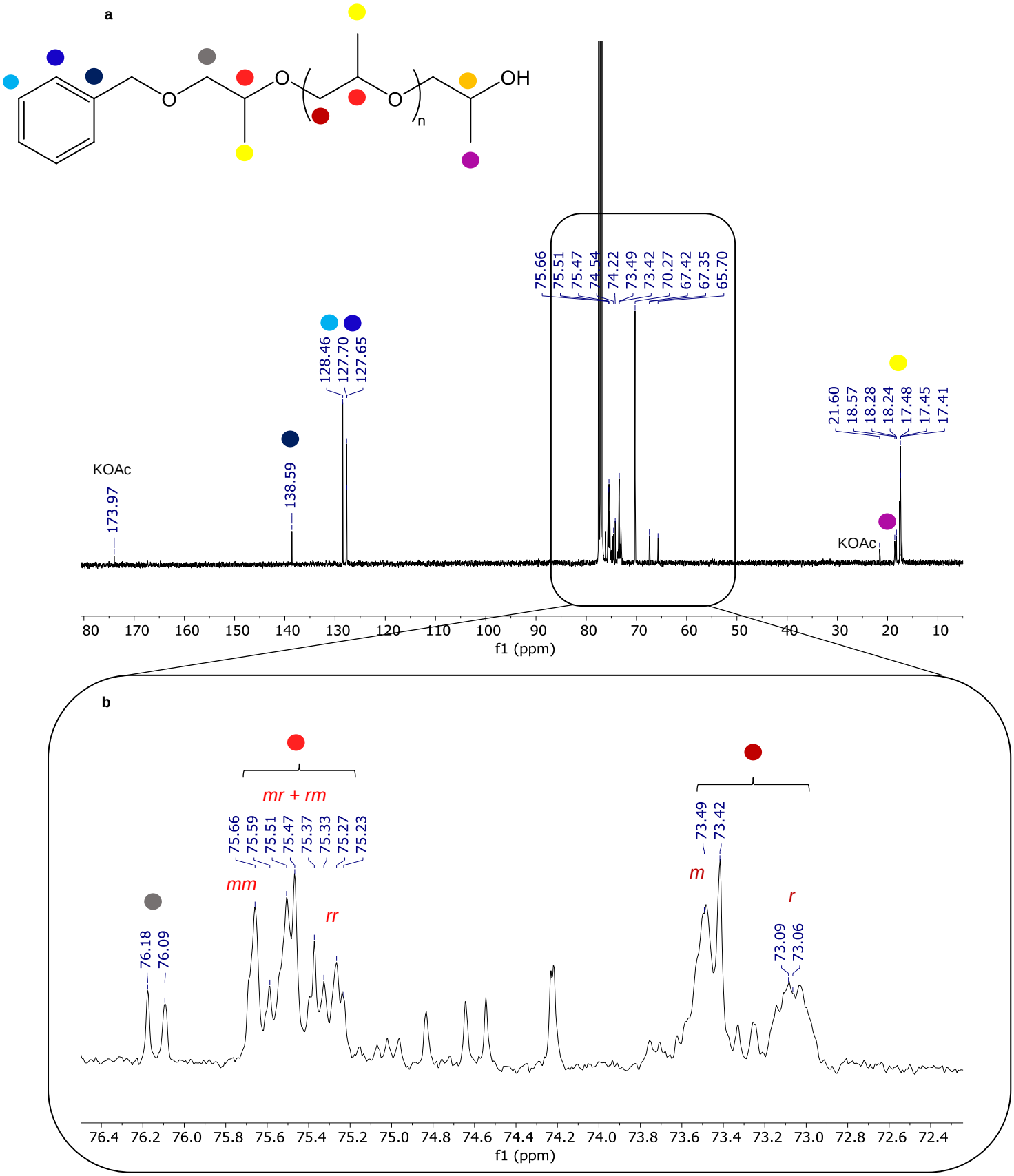

Supplementary Figure 5. (**a**) ^{13}C NMR spectrum ($CDCl_3$, 101 MHz) of the crude PPO (**b**) zoom of methine and methylene regions of atactic PPO. The *m* and *r* refer to the meso and racemic.

3.5. ^{1}H and ^{13}C NMR spectra of PAGE.

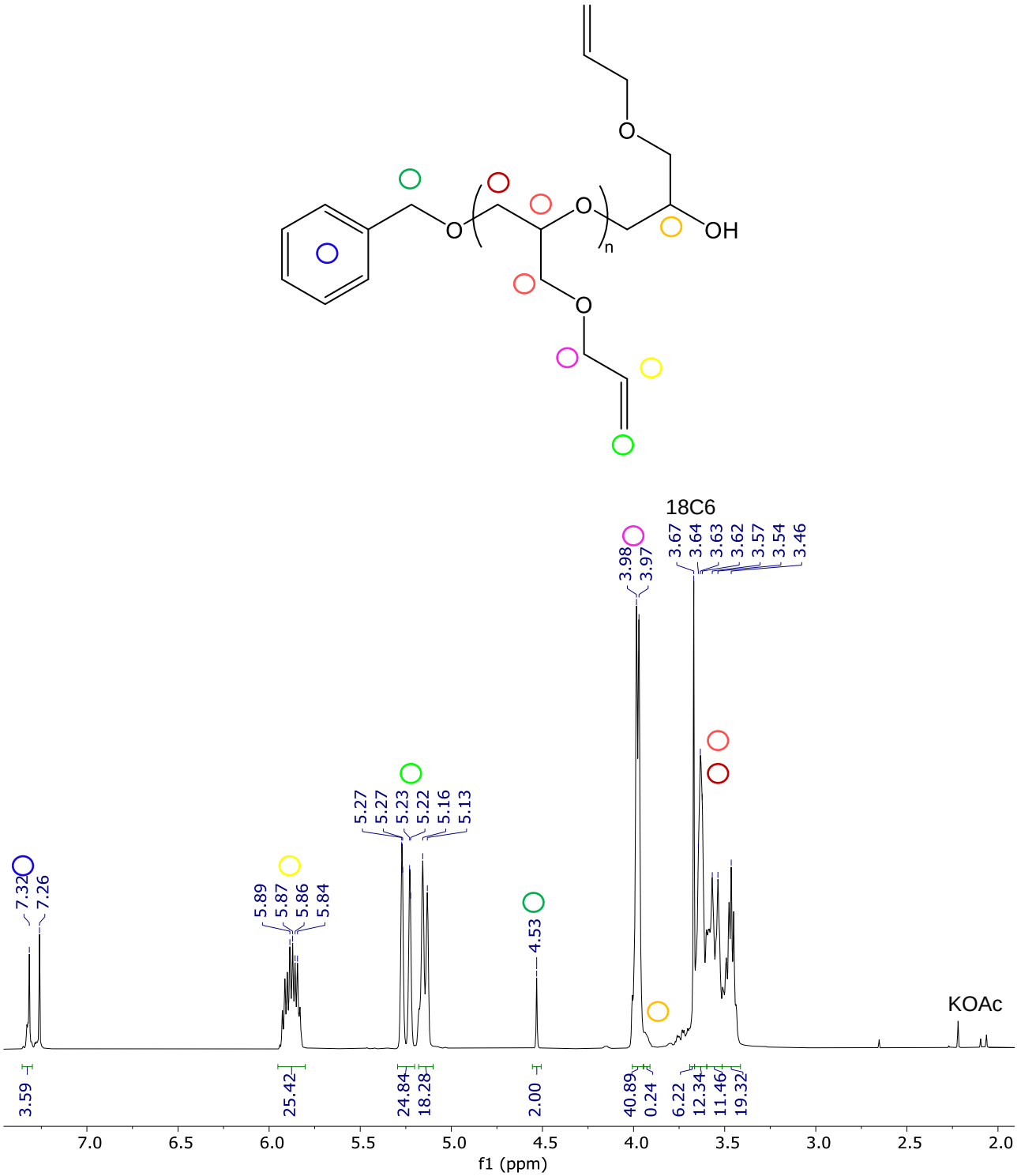

Supplementary Figure 6. ^{1}H NMR spectrum ($CDCl_3$, 400 MHz) of the crude PAGE after full conversion. Condition: $[AGE]_0/[BnOH]_0/[18C6/KOAc]_0$ = 25/1/0.5.

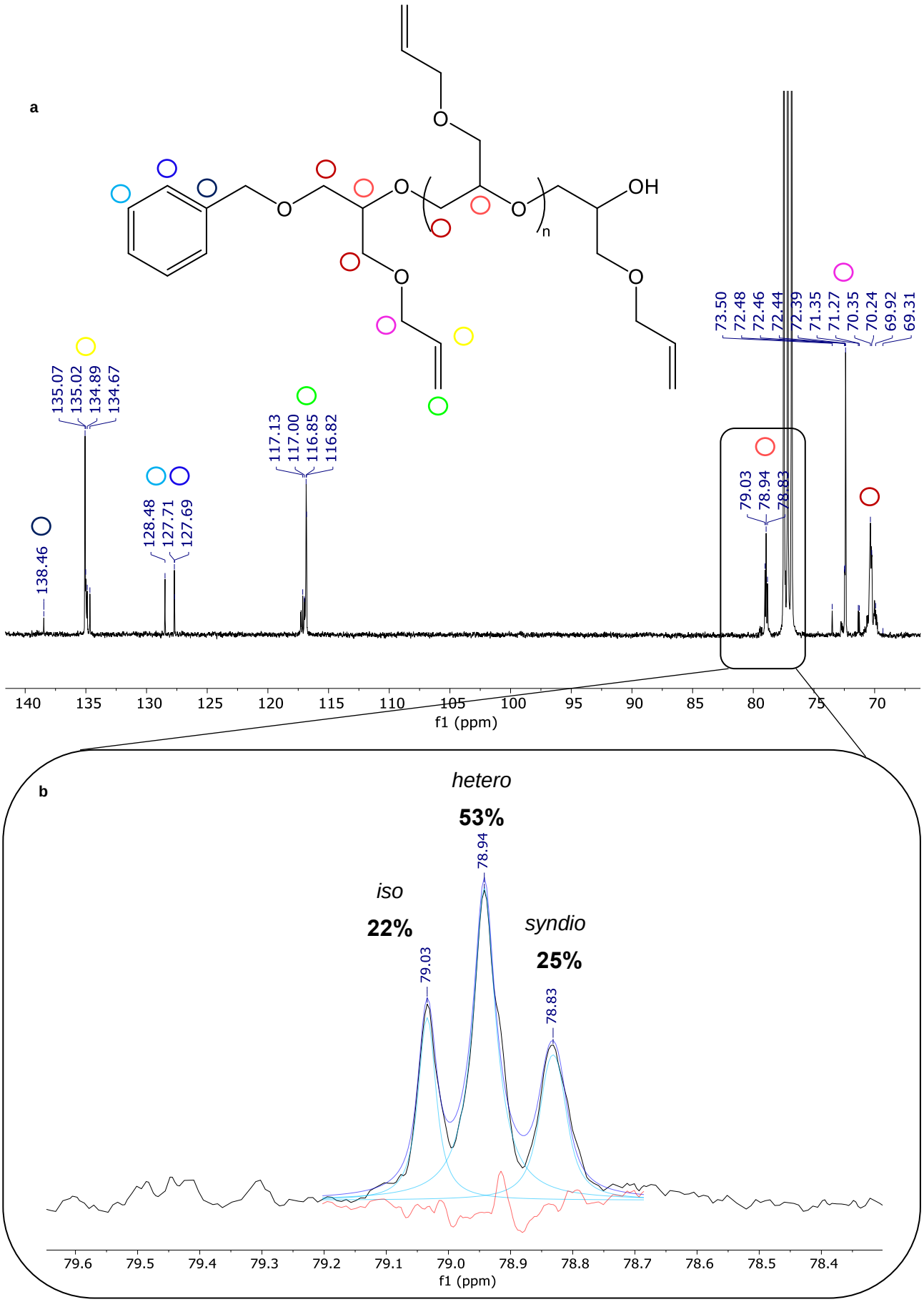

Supplementary Figure 7. (**a**) ^{13}C NMR spectrum ($CDCl_3$, 101 MHz) of the crude PAGE (**b**) with a focus on the region between 78.83 and 79.03 ppm that corresponds to the backbone methine carbon.

3.6. SEC traces of PO and AGE homopolymerizations from iPrOH.

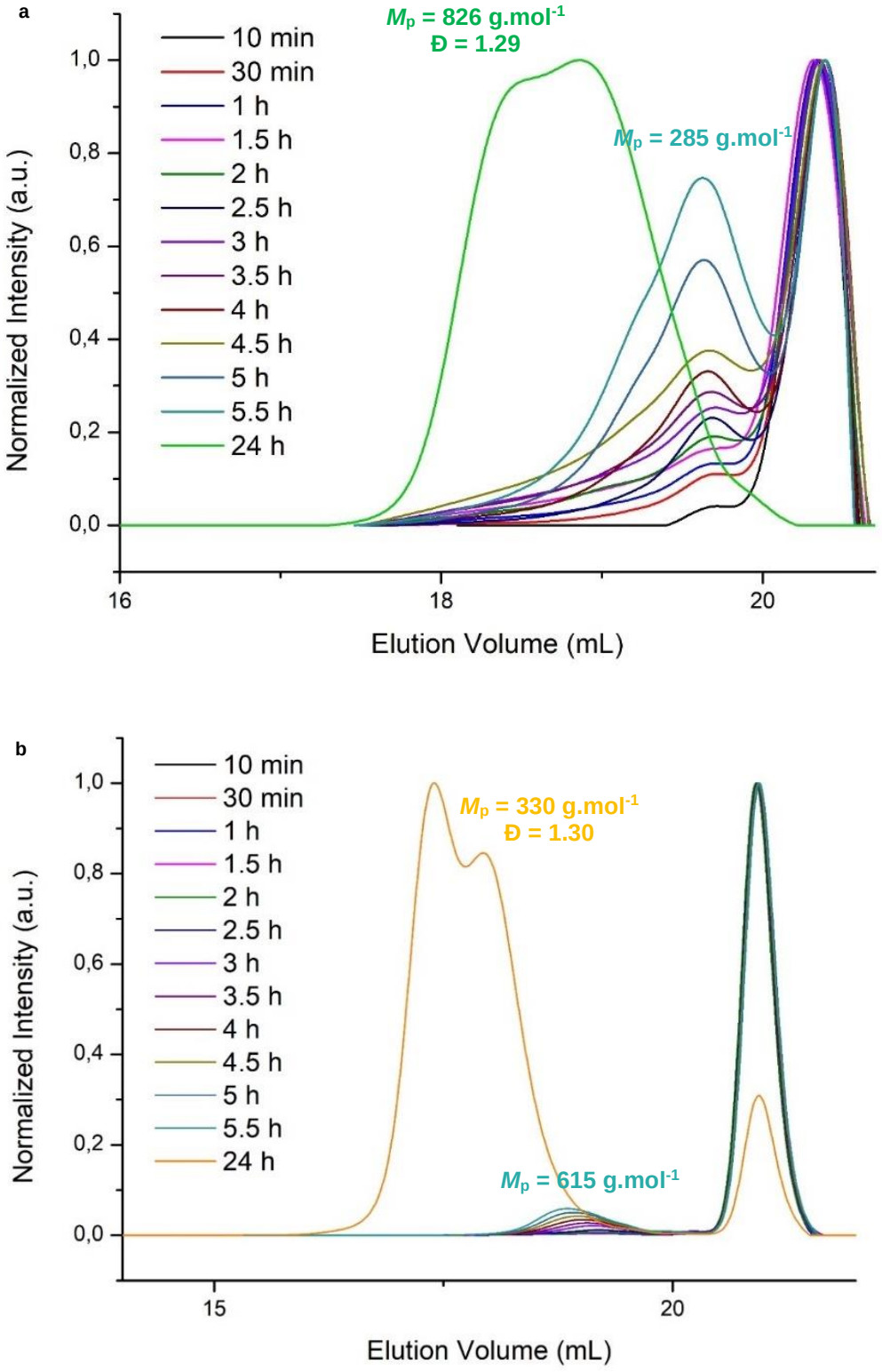

Supplementary Figure 8. Evolution of SEC traces in homopolymerizations of PO (**a**) and AGE (**b**) initiated with iPrOH. Conditions: $[M]_0/[iPrOH]_0/[18C6/KOAc]_0$ = 25/1/0.5.

3.7. Overlay ^{1}H spectra of PO and AGE mixtures.

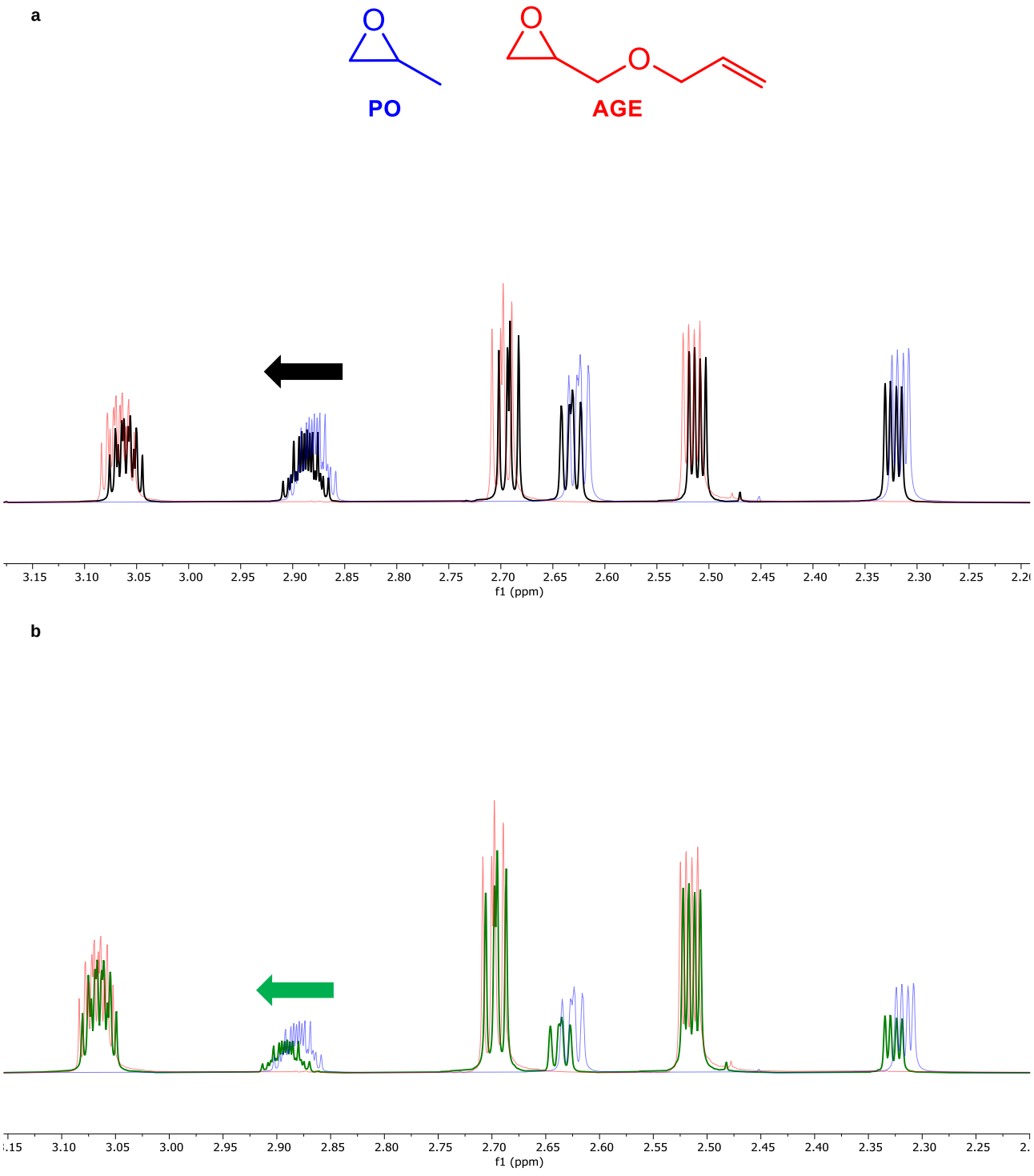

Supplementary Figure 9. Overlay ^{1}H NMR spectra (THF-d_8, 500 MHz) of several mixtures (**a**) $[PO]_0/[AGE]_0$ = 1 (black spectrum), (**b**) $[PO]_0/[AGE]_0$ = 0.5 (green spectrum) with PO (blue spectrum) and AGE (red spectrum). Total mixture concentrations of [PO], [AGE] and [PO+AGE] = 8.6 M in THF-d_8.

3.8. Kinetic plots of PO and AGE copolymerizations.

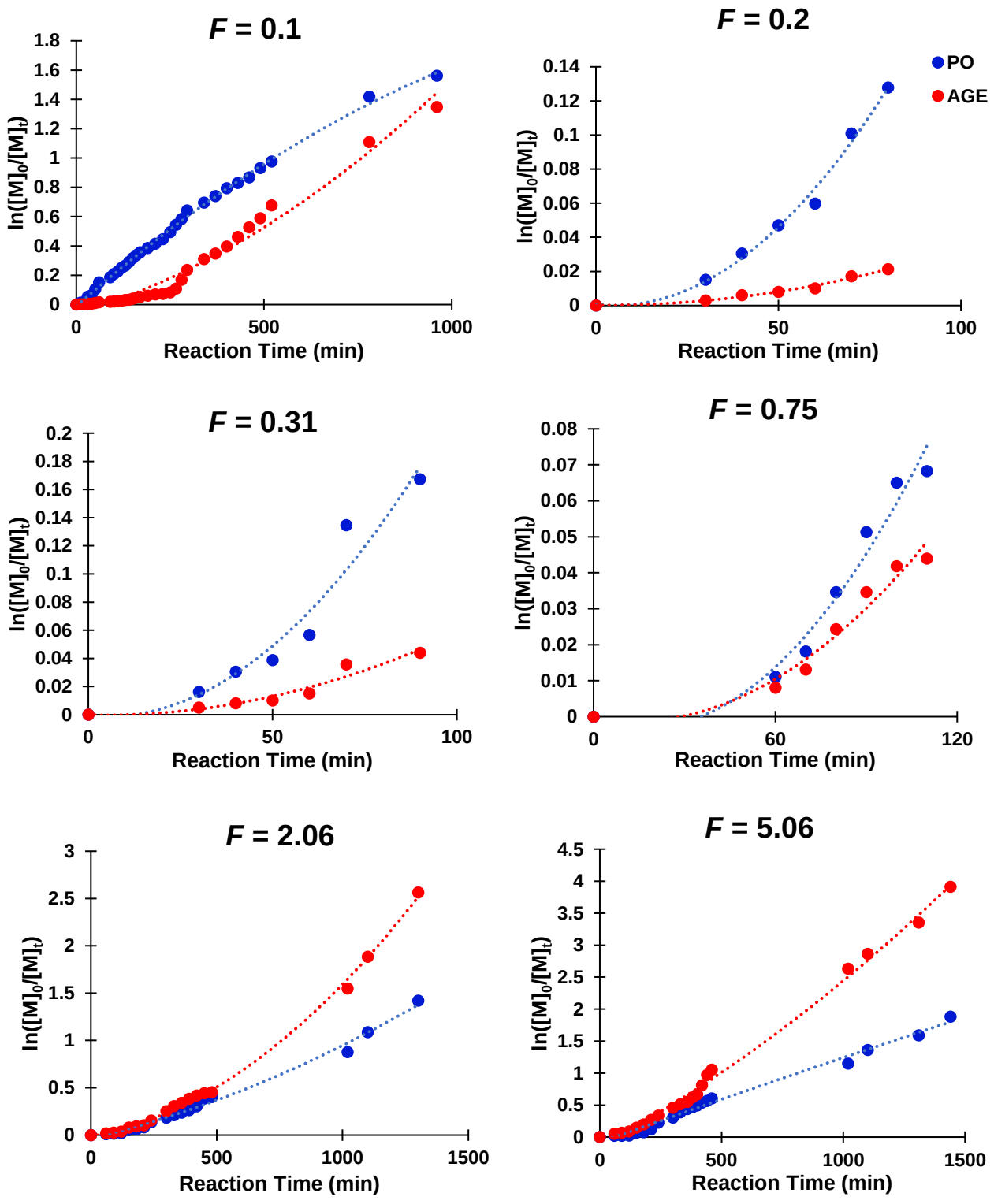

Supplementary Figure 10. Time dependence of the global conversion in the statistical copolymerization of PO and AGE at different molar fraction of PO. Associated semilogarithmic plots ($[M]_t$ measured by ^1H NMR spectroscopy, 500 MHz). The kinetic measurements were started after 30 minutes for $F < 1$, and after 60 minutes for $F > 1$, while each spectrum was recorded in a range of 10-20 minutes. Details of spectra acquisition: 10-15 mg of copolymer in 0.6 mL of $CDCl_3$, number of scans = 128.

3.9. ^{1}H and ^{13}C NMR spectra of P(PO-*co*-AGE) copolymers.

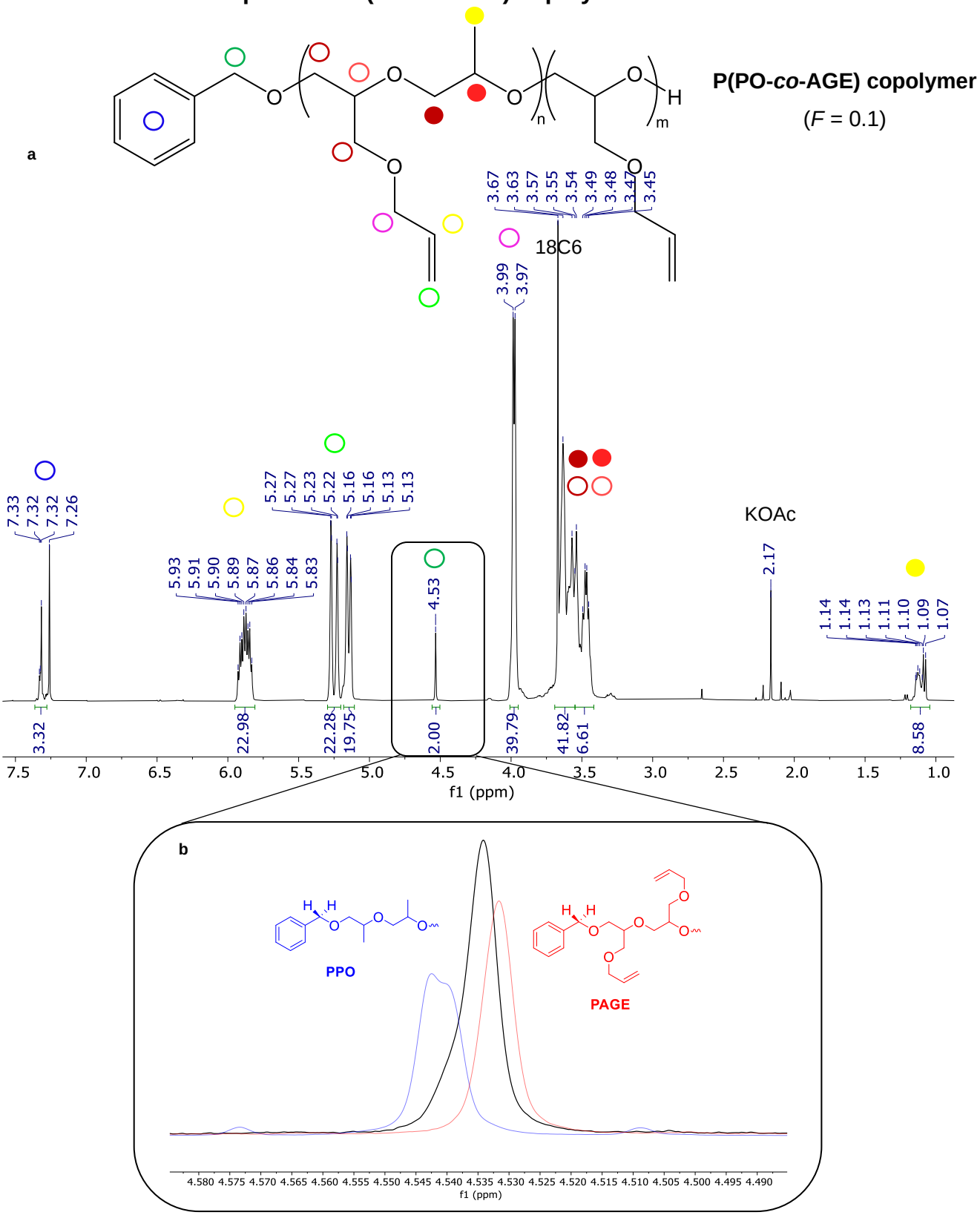

Supplementary Figure 11. (**a**) ^{1}H NMR spectrum ($CDCl_3$, 400 MHz) of P(PO-*co*-AGE) crude media. Conditions: $[PO+AGE]_0/[BnOH]_0 = 25$ with *F* of 0.1 after full conversion. (**b**) overlay ^{1}H NMR spectra to compare the α-phenyloxy end-groups of P(PO-*co*-AGE) (black spectrum) with the end-groups of PAGE (red spectrum) and PPO (blue spectrum).

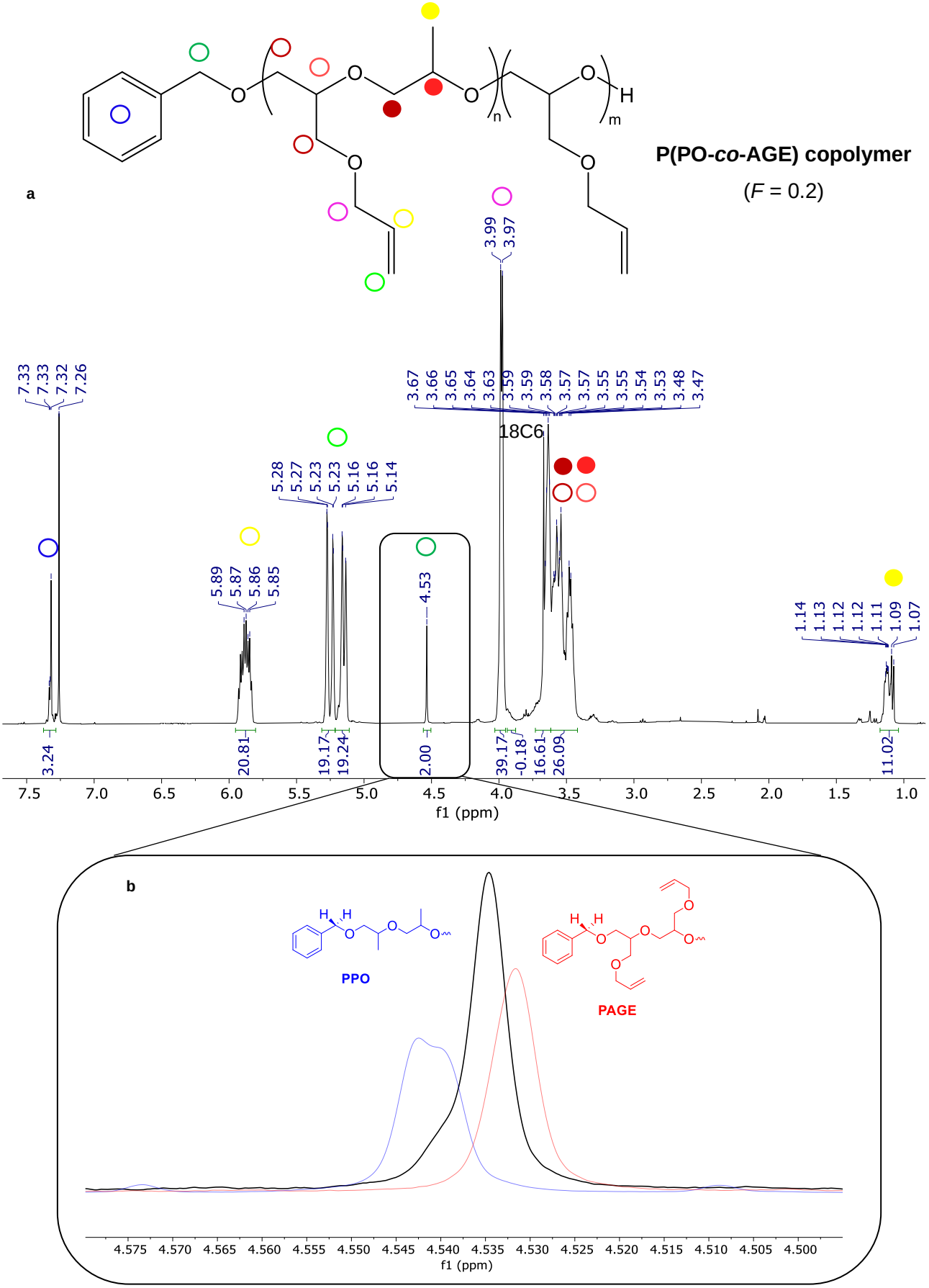

Supplementary Figure 12. (**a**) ^{1}H NMR spectrum ($CDCl_3$, 400 MHz) of P(PO-*co*-AGE) crude media. Conditions: $[PO+AGE]_0/[BnOH]_0 = 25$ with *F* of 0.2 after full conversion. (**b**) overlay ^{1}H NMR spectra to compare the α-phenyloxy end-groups of P(PO-*co*-AGE) (black spectrum) with the end-groups of PAGE (red spectrum) and PPO (blue spectrum).

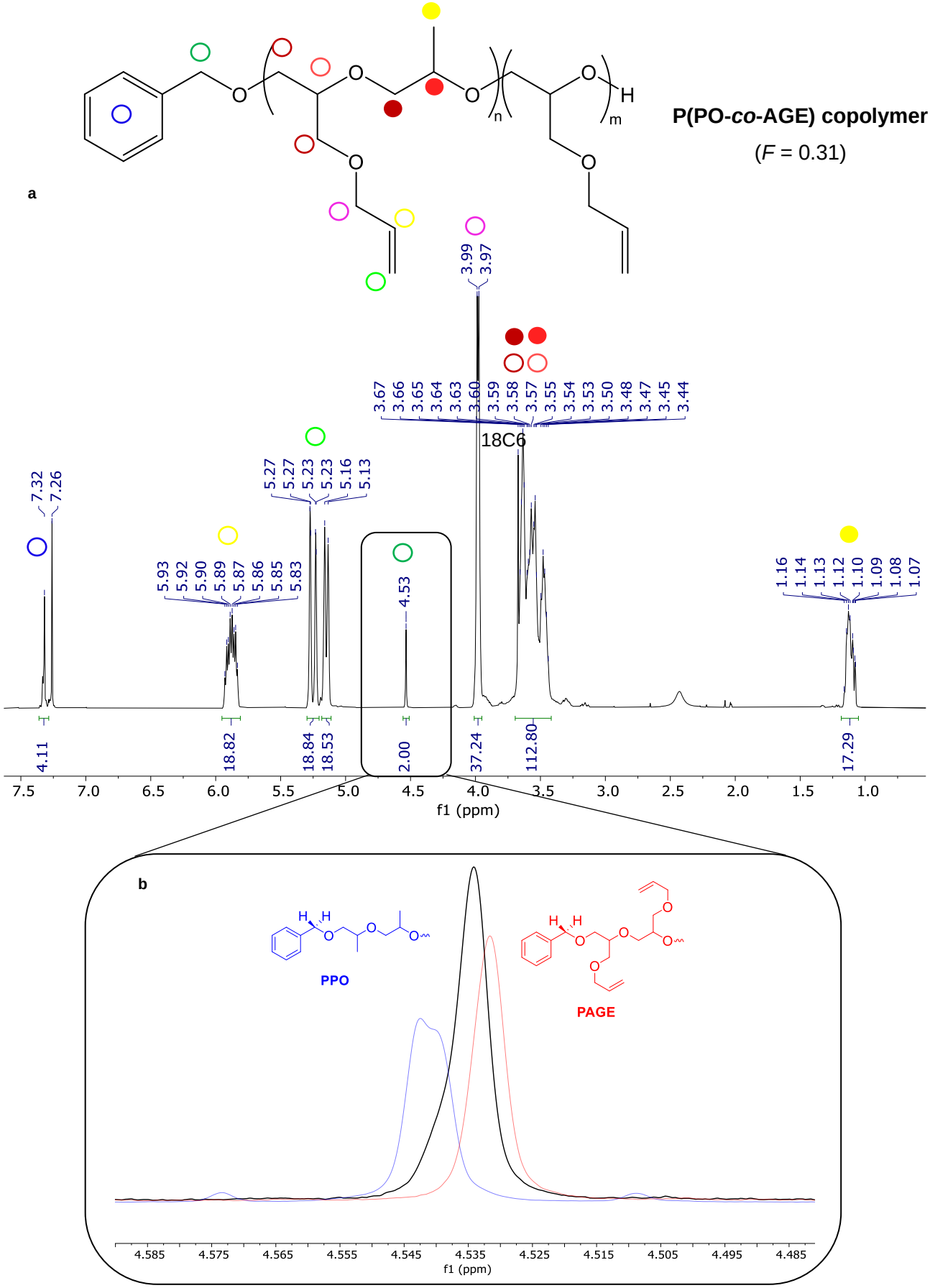

Supplementary Figure 13. (**a**) ^{1}H NMR spectrum ($CDCl_3$, 400 MHz) of P(PO-*co*-AGE) crude media. Conditions: $[PO+AGE]_0/[BnOH]_0$ = 25 with *F* of 0.31 after full conversion. (**b**) overlay ^{1}H NMR spectra to compare the α-phenyloxy end-groups of P(PO-*co*-AGE) (black spectrum) with the end-groups of PAGE (red spectrum) and PPO (blue spectrum).

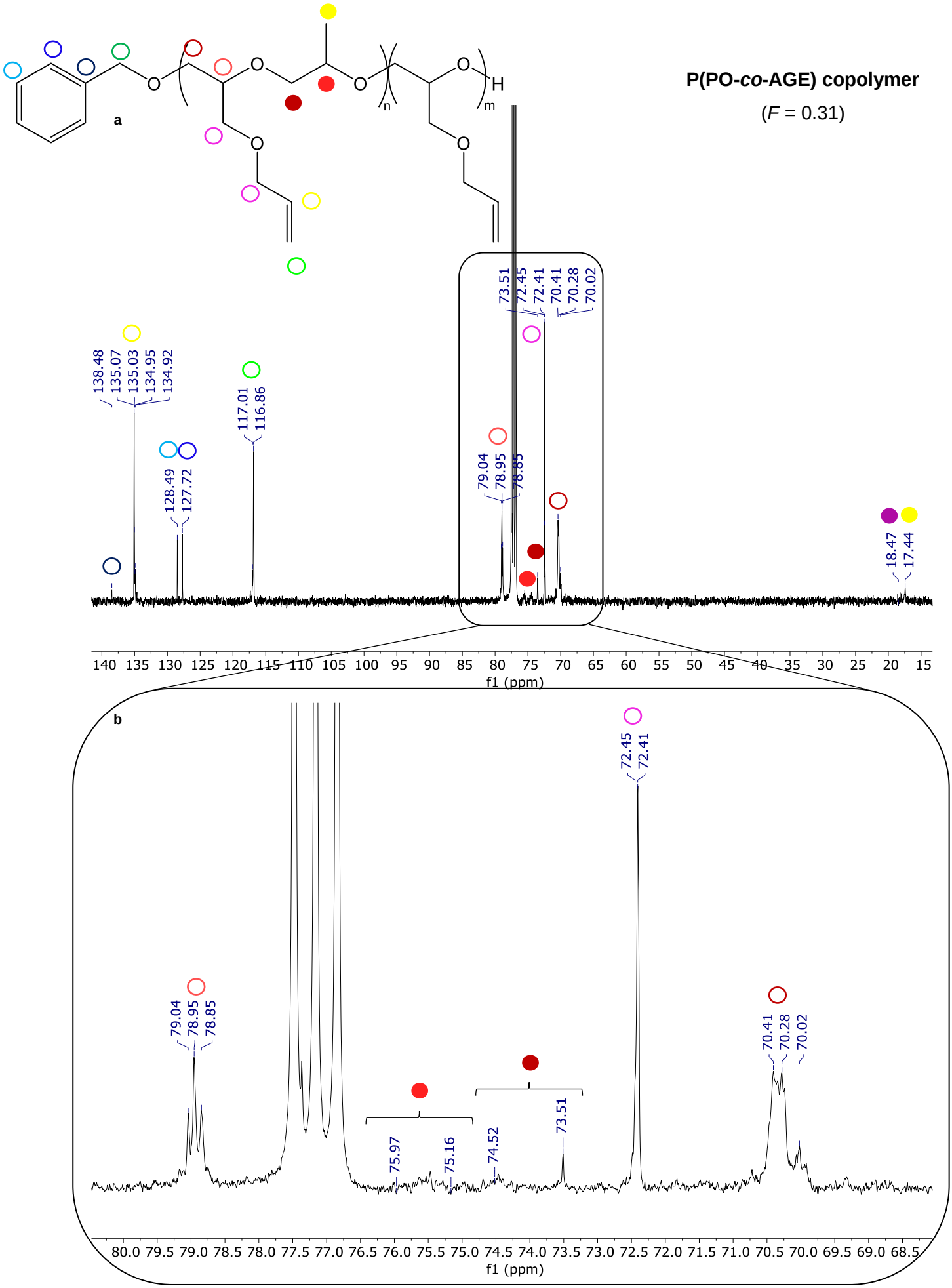

Supplementary Figure 14. (**a**) ^{13}C NMR spectrum ($CDCl_3$, 400 MHz) of P(PO-*co*-AGE) crude media (**b**) with a focus on the methine and methylene regions of P(PO-*co*-AGE) copolymer.

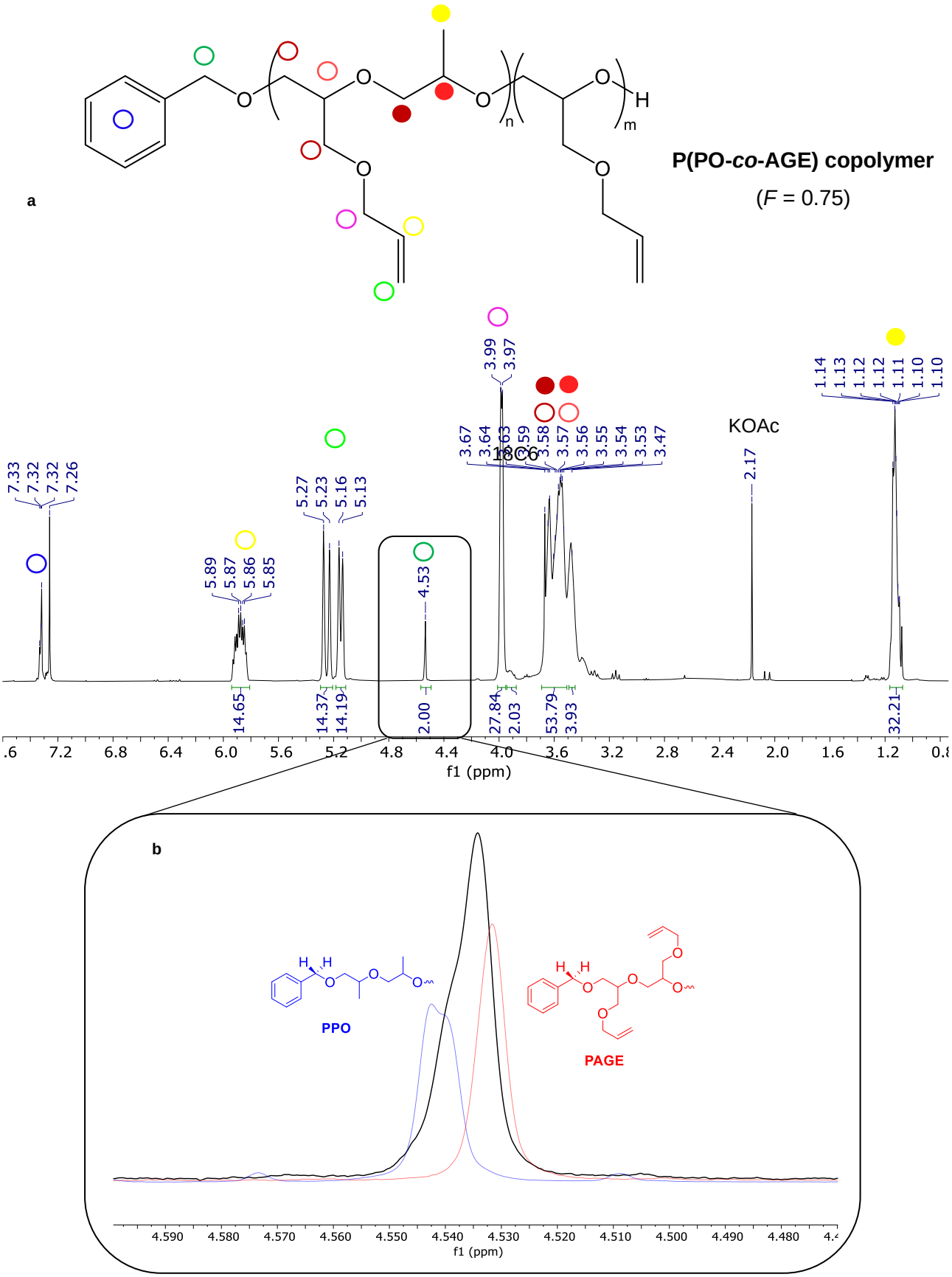

Supplementary Figure 15. (**a**) ^{1}H NMR spectrum ($CDCl_3$, 400 MHz) of P(PO-*co*-AGE) crude media. Conditions: $[PO+AGE]_0/[BnOH]_0$ = 25 with *F* of 0.75 after full conversion. (**b**) overlay ^{1}H NMR spectra to compare the α-phenyloxy end-groups of P(PO-*co*-AGE) (black spectrum) with the end-groups of PAGE (red spectrum) and PPO (blue spectrum).

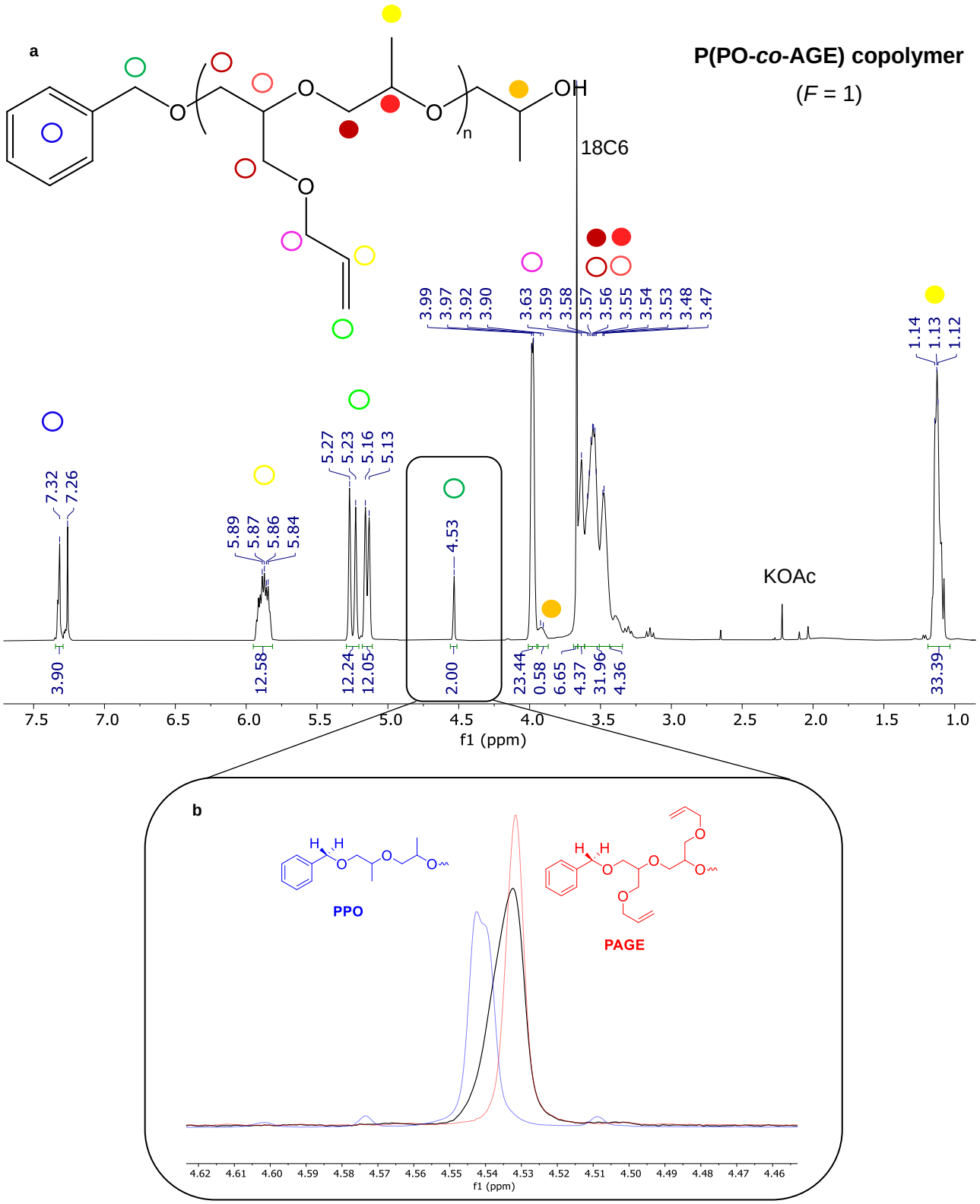

Supplementary Figure 16. (**a**) ^{1}H NMR spectrum ($CDCl_3$, 400 MHz) of P(PO-*co*-AGE) crude media. Conditions: $[PO+AGE]_0/[BnOH]_0$ = 25 with *F* of 1 after full conversion. (**b**) overlay ^{1}H NMR spectra to compare the α-phenyloxy end-groups of P(PO-*co*-AGE) (black spectrum) with the end-groups of PAGE (red spectrum) and PPO (blue spectrum).

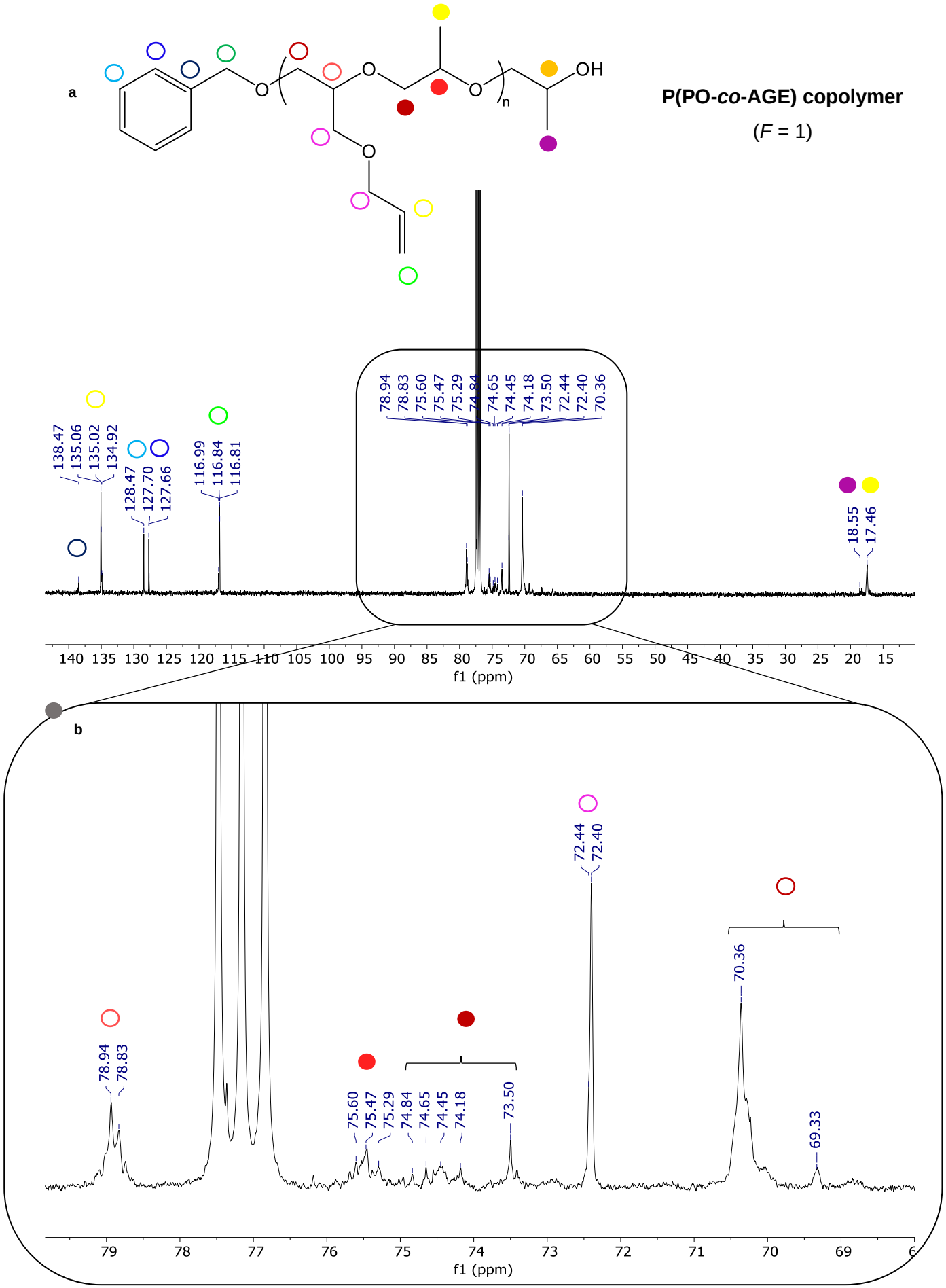

Supplementary Figure 17. (**a**) ^{13}C NMR spectrum ($CDCl_3$, 400 MHz) of P(PO-*co*-AGE) crude media (**b**) with a focus on the methine and methylene regions of P(PO-*co*-AGE) copolymer.

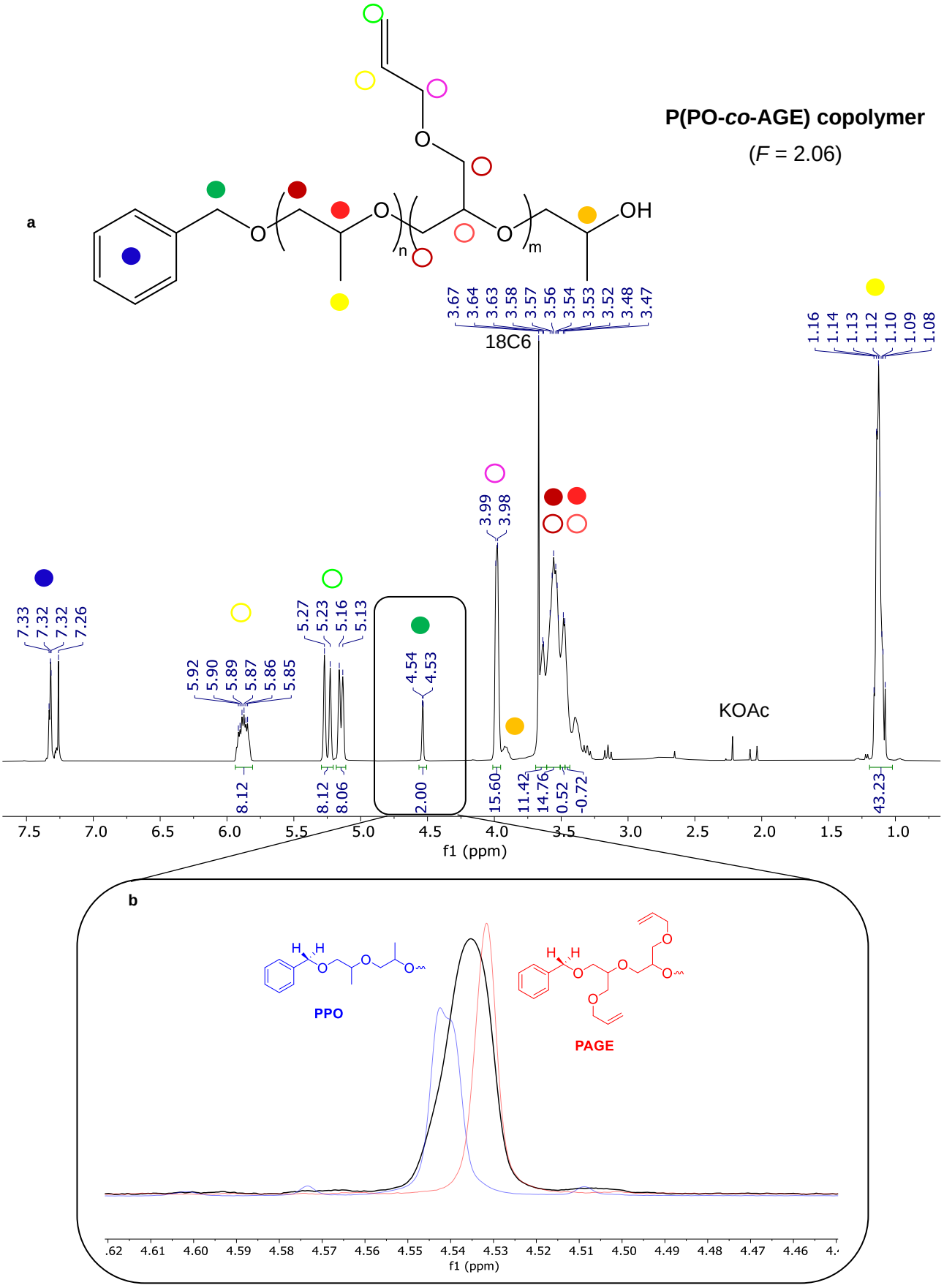

Supplementary Figure 18. (**a**) ^{1}H NMR spectrum ($CDCl_3$, 400 MHz) of P(PO-*co*-AGE) crude media. Conditions: $[PO+AGE]_0/[BnOH]_0$ = 25 with *F* of 2.06 after full conversion. (**b**) overlay ^{1}H NMR spectra to compare the α-phenyloxy end-groups of P(PO-*co*-AGE) (black spectrum) with the end-groups of PAGE (red spectrum) and PPO (blue spectrum).

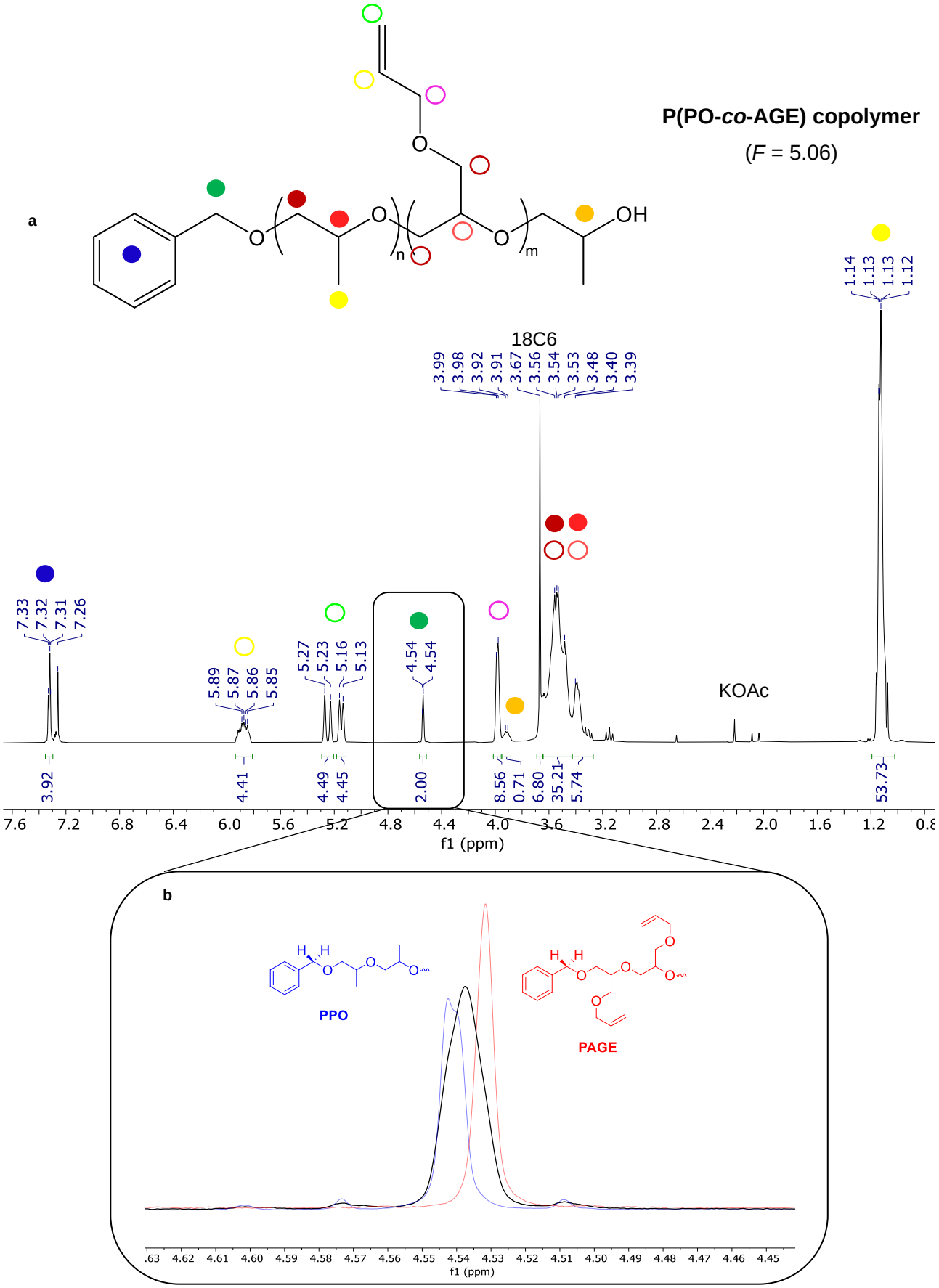

Supplementary Figure 19. (**a**) ^{1}H NMR spectrum ($CDCl_3$, 400 MHz) of P(PO-*co*-AGE) crude media. Conditions: $[PO+AGE]_0/[BnOH]_0$ = 25 with *F* of 5.06 after full conversion. (**b**) overlay ^{1}H NMR spectra to compare the α-phenyloxy end-groups of P(PO-*co*-AGE) (black spectrum) with the end-groups of PAGE (red spectrum) and PPO (blue spectrum).

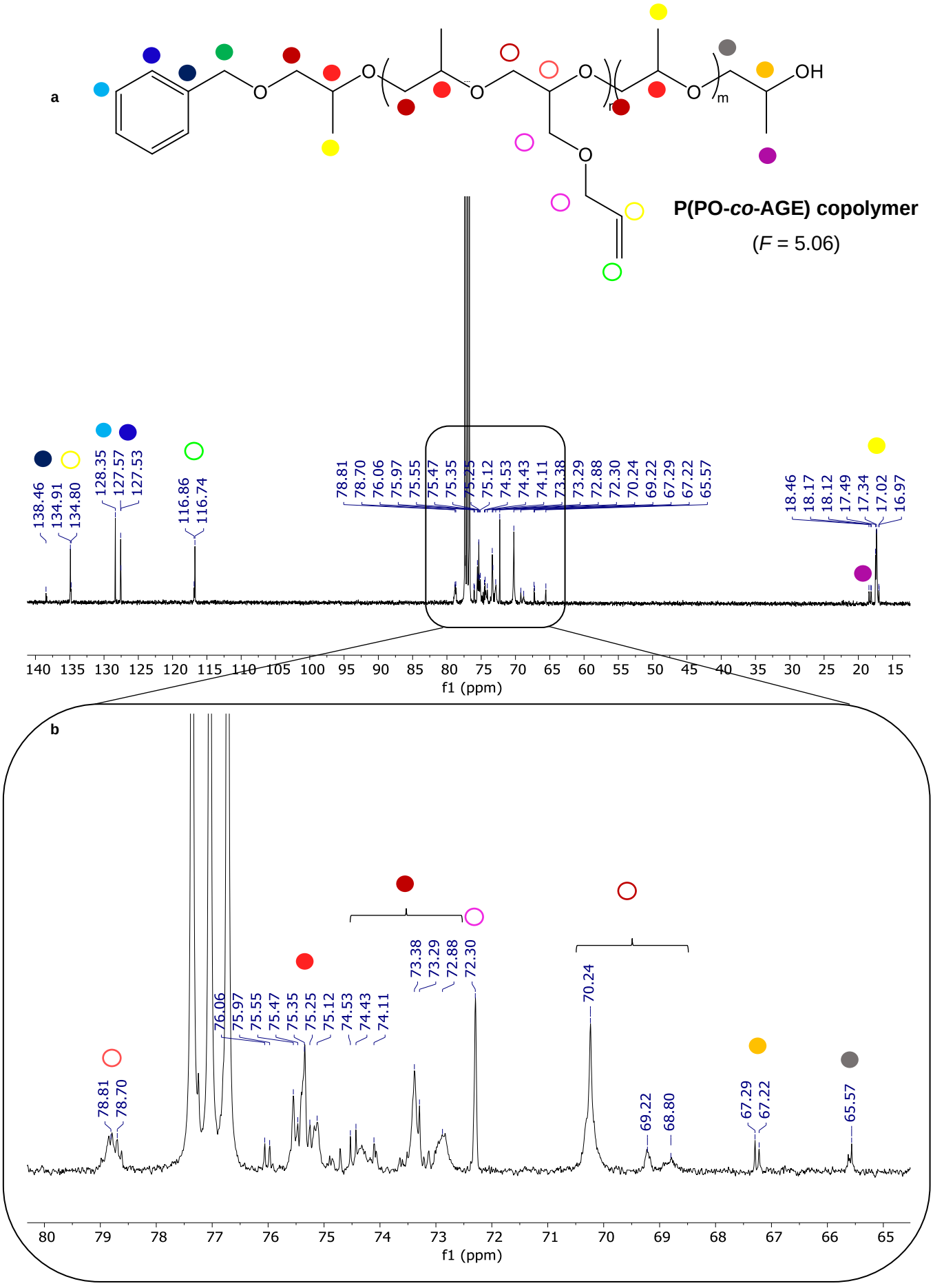

Supplementary Figure 20. (**a**) ^{13}C NMR spectrum ($CDCl_3$, 400 MHz) of P(PO-*co*-AGE) crude media (**b**) with a focus on the methine and methylene regions of P(PO-*co*-AGE) copolymer.

3.10. Fineman-Ross copolymerization equation.

$$y = r_1 \cdot x + r_2$$

$$y = \frac{f_1(1 - 2 \cdot F_1)}{(1 - f_1) \cdot F_1} \qquad x = \frac{{f_1}^2(F_1 - 1)}{(1 - f_1)^2 \cdot F_1}$$

$$F_1 = \frac{d(m_1)}{d(m_1) + d(m_2)} \qquad f_1 = \frac{[M_1]}{[M_1] + [M_2]}$$

Supplementary Figure 21. Fineman-Ross copolymer composition equation used to extrapolate the reactivity ratios between co-monomers. For this purpose, the copolymerization of the co-monomers with different compositions (*F* ($[PO]_0/[AGE]_0$) of 0.1, 0.2, 0.31, 0.75, 2.06 and 5.06) were performed and the monomer composition in the obtained oligomers was examined at low conversion.

4. Supplementary References

1. Akkermans, R. L. C., Spenley, N. A. & Robertson, S. H. COMPASS III: automated fitting workflows and extension to ionic liquids. *Molecular Simulation*. **47**, 540–551 (2021).
2. Fornaciari, C., Pasini, D. & Coulembier, O. Controlled Oxyanionic Polymerization of Propylene Oxide: Unlocking the Molecular-Weight Limitation by a Soft Nucleophilic Catalysis. *Macromol. Rapid Commun*. **43**, 2200424; 10.1002/marc.202200424 (2022).
3. Childers, M. I., Longo, J. M., Van Zee, N. J., LaPointe, A. M. & Coates, G. W. Stereoselective Epoxide Polymerization and Copolymerization. *Chem. Rev*. **114**, 8129−8152 (2014).
4. Rodriguez, C.G., Ferrier, R.C., Helenic, A. & Lynd, N.A. Ring-Opening Polymerization of Epoxides: Facile Pathway to Functional Polyethers via a Versatile Organoaluminum Initiator. *Macromolecules*. **50**, 3121–3130 (2017).
5. Fineman, M. & Ross, S. D. Linear method for determining monomer reactivity ratios in copolymerization. *J. Polym. Sci*. **5**, 259–262 (1959).